We are IntechOpen,
the world's leading publisher of
Open Access books
Built by scientists, for scientists

6,900
Open access books available

185,000
International authors and editors

200M
Downloads

154
Countries delivered to

Our authors are among the

TOP 1%
most cited scientists

12.2%
Contributors from top 500 universities

CLARIVATE ANALYTICS

BOOK CITATION INDEX

INDEXED

WEB OF SCIENCE™

Selection of our books indexed in the Book Citation Index
in Web of Science™ Core Collection (BKCI)

Interested in publishing with us?
Contact book.department@intechopen.com

Numbers displayed above are based on latest data collected.
For more information visit www.intechopen.com

Absorption Kinetics of Phenol into Different Size Nanopores Present in Syndiotactic Polystyrene and Poly (p-methylstyrene)

Kenichi Furukawa and Takahiko Nakaoki

Additional information is available at the end of the chapter

1. Introduction

The stereoregularity of polyolefins is one of their important characteristics that regulate their physical properties. Since Natta et al. successfully synthesized isotactic polypropylene having high stereoregularity,[1] many investigations have been reported, not only from the viewpoint of stereoregular polymerization, but also with regard to the molecular structure based on the stereoregularity. Isotactic polystyrene (iPS) is one of the earliest stereoregular polymers synthesized using the Ziegler-Natta catalyst in 1955.[2] The stereoregular repeating unit allows it to form a crystal with 3/1 helical structure. Syndiotactic polystyrene (sPS), the counterpart of iPS, was first synthesized by Ishihara et al. in 1986.[3]

One of the most attractive features of this material is that there exists polymorphic structures. It has been reported that there are five crystalline modifications. The α [4-8] and β [9, 10] forms consist of a planar zigzag chain with period of 5.1 Å, whereas the γ [11-13], δ [14-17], and ϵ [18-20] forms adopt a helical structure with a trans-trans-gauche-gauche (ttgg) conformation, having a period of 7.7 Å. The crystal with an all-trans conformation is a thermally stabilized form induced above about 180 °C and its high melting temperature around 270 °C is expected to be useful as an engineering plastic. The ttgg conformation is induced by the presence of organic solvents such as aromatic and chlorinated compounds and crystals of both the δ- and ϵ-forms are characterized by the formation of complex structures containing solvent molecules. The difference between these crystalline forms is that δ-sPS is formed by casting from solution or exposing it to the vapor of organic compound, whereas ϵ-sPS is formed by treating γ-sPS in chloroform. The molecular dipoles of guest molecules in the crystal units are respectively perpendicular and parallel to the chain axis of δ- and ϵ-sPS. It is worth noting that a nanoporous structure in these crystals

can be prepared by removing the incorporated solvent in acetone or supercritical carbon dioxide (scCO2). [21-25]

Similar molecular structures have been reported for syndiotactic poly(*p*-methylstyrene) (sPPMS); the all-trans conformation (forms III, IV, and V) induced by annealing, and the ttgg conformation (forms I and II) induced by organic solvents. [26-28] In addition, three clathrate forms of α-, β-, and γ-classes which contain solvent in the crystal unit have been reported. The α and β class clathrates have a ttgg conformation with a period of 7.8 ± 0.1 Å. [29-32]The $t_6g_2t_2g_2$ conformation γ class clathrate has a period of 11.7 ± 0.1 Å. [33] A porous crystalline structure can be constructed in a crystal with the ttgg conformation by removing the solvent. However, this solvent-depleted crystal is unstable, being readily collapsed on removing the solvent.[34]

One of the most important features of sPS and sPPMS is their abilities to form nanoporous structures. The nanoporous structure of δ_e-sPS, in particular, is a very attractive morphology for the absorption of specific compounds. Many investigations have been carried out on the sorption and desorption kinetics of liquid organic compounds, such as 1,2-dichloroethane, and also gases such as CO_2. [35, 36] The absorption rate of solvent molecules was enhanced by a porous aerogel with **a** mesh structure, which was prepared by treating the sPS gel in scCO2.[37-39] The relationship between the size of the solvent molecule and the cavity volume of δ_e-sPS was reported by Tsujita et al. [40-43] It was shown that the cavity volume of δ-sPS is reduced after extracting the solvent molecules.

Our research group reported that the pore dimension can be regulated by the size of the solvent molecule, being larger for solvents with a larger molar volume. Furthermore, the absorption of linear and branched alcohols with four and five carbons depended on the molecular shape. [44] The alcohols with a bulk substituent, such as a methyl group, were impossible to incorporate in the pore because of their bulk. In addition, the absorption process of ethanol and butanols for sPS and sPPMS was investigated from the viewpoint of the pore size in the crystal. [34] The diffusion of ethanol into the large cavity pores of sPPMS was faster than that of sPS. A bulky alcohol, such as *tert*-butanol, was not absorbed by sPS but did incorporate into sPPMS.

Our previous report concerned aliphatic alcohols.[44] In this report, the absorption of phenol in nanoporous crystals of sPS and sPPMS is investigated.

2. Experimental section

The sPS was supplied by Idemitsu Petrochemical Co. Ltd. The weight average molecular weight (M_w) and polydispersity (M_w/M_n) were 2.4×10^5 and 2.3, respectively. The sPPMS was prepared using tetramethylcyclopentadienyl titanium trichloride (Cp*TiCl3) and methylaluminoxane (MAO) as a polymerization catalyst. The weight average molecular weight (M_w) and polydispersity (M_w/M_n) were 5.8×10^5 and 1.6, respectively. Films of the two polymers were prepared as follows. A melt-quenched film was obtained by quenching in ice-water after melting at 280 °C. A cast-crystallized film was obtained by treating the film cast from *m*-xylene solution with scCO2. As described in our previous paper, [34] the cast-

crystallized sPS and sPPMS from m-xylene adopt the δ_e-form and form I, respectively. The treatment in scCO₂ was performed using a supercritical fluid apparatus (Jasco SCF-Get) under the mild conditions of 40 °C and 10 MPa. Sorption of phenol was carried out by soaking the sPS or sPPMS film a 5% aqueous solution of phenol.

Infrared spectra were measured on a JASCO FT-IR660 Plus over the standard wavenumber range of 400 - 4000 cm^{-1}. The film thickness was calibrated by the Lambert-Beer equation as follows.

$$A = \varepsilon \cdot c \cdot l \tag{1}$$

Here A, ε, c, and l denote the absorbance, absorption coefficient, molar concentration, and the path length, respectively. The following relationship between the absorbance and the film thickness was reported for sPS using the CH out-of-plane mode of the phenyl ring at 1028cm^{-1} as an internal standard.[44]

$$A_{1028} = 1.004 \times 10^{-2} \cdot l \tag{2}$$

In order to calibrate the film thickness for sPPMS, the 1022 cm^{-1} band, which does not depend on the crystalline form, was used. Figure 1 shows the absorbance of melt-quenched sPPMS at 1022 cm^{-1} against the film thickness, which was determined by a micrometer. The slope provided the following relationship.

$$A_{1032} = 1.010 \times 10^{-2} \cdot l \tag{3}$$

From these relationships, the film thickness of sPS and sPPMS were estimated, respectively.
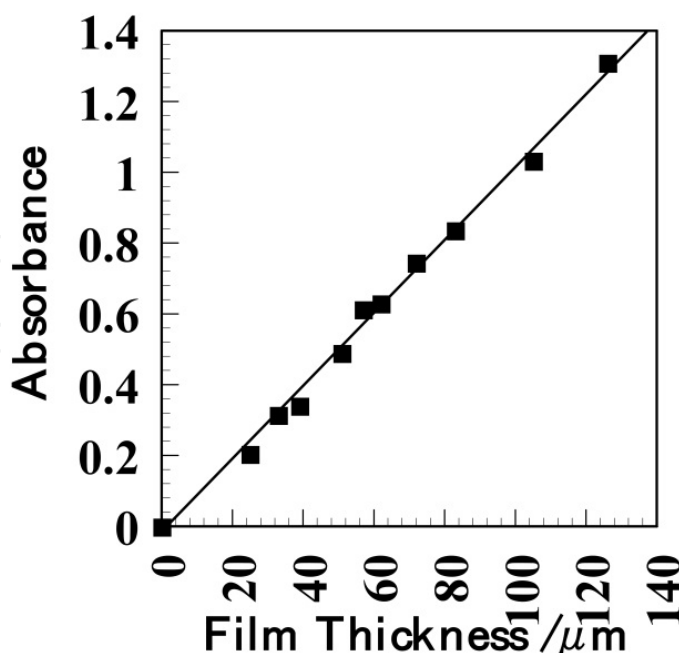

Figure 1. Dependence of the absorbance of the OH stretching mode for phenol on path length. Nakaoki et al.

The degree of crystallinity was estimated by a flotation method. Water and *tert*-butanol were used for sPS as a mixed solvent. In the case of sPPMS, solvents with large molar volume such as 3-ethyl-3-pentanol and dimethysulfoxide (DMSO) were used as a mixed solvent. We confirmed by infrared spectroscopy that these solvents were not absorbed in the polymer films. The density was determined by a Lipkin-type pyknometer at 25 °C. The measurements were carried out three times and the average value was taken to estimate the crystallinity. The following equation was used to determine the crystallinity (χ_C).

$$\chi_C = \frac{\rho - \rho_C}{\rho_a - \rho_C} \qquad (4)$$

Here ρ_C and ρ_a denote the densities of crystalline and amorphous material, respectively and ρ is the observed density.

3. Results and discussion

3.1. Absorption of phenol into the pores in crystals of sPS and sPPMS

The sPS and sPPMS films were soaked in phenol solution for one week, and the infrared spectrum was remeasured. Figure 2 shows the infrared spectrum of the OH stretching mode of phenol. The absorption peak at 3540 cm^{-1} assignable to the H bond-free OH stretching mode was observed for the cast-crystallized sPS and sPPMS. This indicates that there is no interaction between phenol molecules, because each phenol molecule is isolated in a pore of the sPS and sPPMS crystal. Contrary to the cast-crystallized films, two peaks were observed for the melt-quenched films. In addition to the peak at 3540 cm^{-1}, a broad absorption peak around 3300 cm^{-1}, which is assignable to the OH stretching mode associated with a hydrogen bond was observed. This indicates that the phenol molecules exist in a non-crystalline region. The fact that the 3540 cm^{-1} band was also observed indicates that the crystallization proceeded to the δ-form, which then incorporated phenol into the crystal.

Figure 3 shows the infrared spectra of the phenyl out-of-plane mode of sPS and sPPMS, before and after soaking in phenol solution. The peaks characteristic of the ttgg conformation at 572 cm^{-1} and 566 cm^{-1} for sPS and sPPMS are well-known to be very sensitive to the conformation. These peaks increased in intensity for both cast-crystallized and melt-quenched films after soaking in phenol solution. This is direct evidence that the crystal with a ttgg conformation was induced by the presence of phenol.

The crystallinity of cast-crystallized δ$_e$-sPS and sPPMS was estimated by the flotation method. The calculated values are listed in Table 1. In general, the crystal takes a tightly packed structure so that the density of the crystal tends to be higher. However the densities of the cast-crystallized sPS and sPPMS films were lower than those of the amorphous polymer, because of the porous structure obtained after excluding solvent molecules. The crystallinity of the cast-crystallized sPPMS was as low as 4.7 %, which is in contrast to that
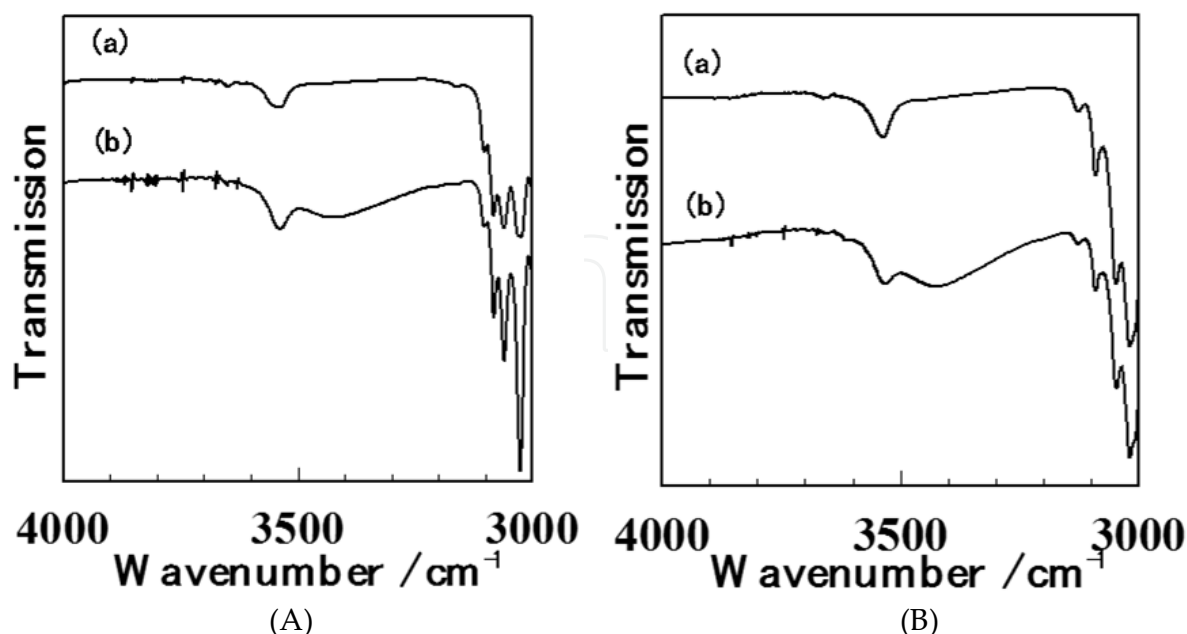
Figure 2. Infrared spectra for the cast-crystallized (a) and melt-quenched (b) sPS (A) and sPPMS (B) after soaking in a 5 wt% phenol aqueous solution for 24 h. The peaks at 3540 cm^{-1} and 3300 cm^{-1} are assignable to the OH stretching mode of phenol without, and with hydrogen bonding, respectively. Nakaoki et al.
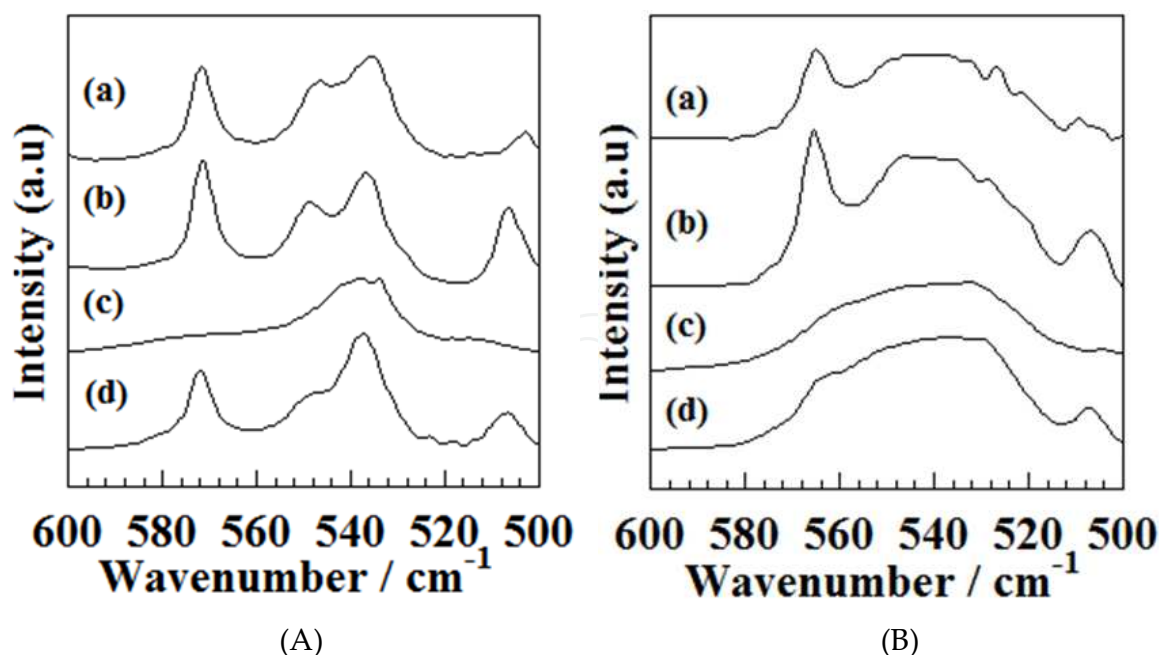

Figure 3. Infrared spectra of sPS (A) and sPPMS (B). The (a) and (b) spectra correspond to the cast-crystallized films before, and after, soaking in a 5 wt% phenol aqueous solution, respectively. The (c) and (d) spectra correspond to the melt-quenched films, before and after, soaking in a 5 wt% phenol aqueous solution, respectively. Nakaoki et al.

	ϱ (observed)	ϱC	ϱA
	g/cm³	g/cm³	g/cm³
sPS	1.003	0.977 [a)]	1.055 [b)]
sPPMS	1.010	0.815 [c)]	1.02 [d)]

a) Ref. 25, b) ref. 45, c) ref. 32 and, d) ref. 31.

Table 1. Densities of cast-crystallized sPS and sPPMS determined by the flotation method.

of sPS at 38 %. As described in our previous paper,[34] a complex structure including a solvent molecule is a stable form for sPPMS, and the crystal would collapse on excluding the solvent. Although the crystallinity of the cast-crystallized sPPMS was very low, a porous structure remained, even after removing the solvent because the hydrogen-bond free OH stretching mode was observed for the cast-crystallized sPPMS, as shown in Fig. 2(B). Since the phenol molecule is incorporated in the crystal unit, the flotation method cannot be used to determine the crystallinity because the phenol comes out from the film. In order to estimate the crystallinity after soaking in phenol solution, the infrared spectrum was measured. As described above, the 572 cm^{-1} and 566 cm^{-1} bands for sPS and sPPMS are very sensitive indicators of the formation of the ttgg conformation in during crystallization. Therefore the relationship of the crystallinity with the absorbance at 572 cm^{-1} for sPS (A_{572}) and 566 cm^{-1} for sPPMS (A_{566}) was estimated as follows.

$$\chi_C(sPS) = 1.66 \times 10^{-2} \cdot A_{572} \tag{5}$$

$$\chi_C(sPPMS) = 8.14 \times 10^{-2} \cdot A_{566} \tag{6}$$

The increase in crystallinity after soaking in phenol solution was estimated using these equations and is shown in Table 2. The crystallinity changed from 38 to 52 % for sPS and from 4.7 % to 6.5 % for sPPMS after soaking in phenol solution. In our previous paper concerning the absorption of aliphatic alcohols in sPS and sPPMS,[34] there was no trace of further crystallization. Phenol is basically a poor solvent for these polymers, but it was established that the crystallization can be promoted by soaking in the phenol solution.

	Crystallinity / %	
	before	after
sPS/*m*-xylene cast	38	52
sPPMS/*m*-xylene cast	4.7	6.5
Melt-quenched sPS	0	7.2
Melt-quenched sPPMS	0	1.3

Table 2. Crystallinity before and after soaking in a 5 % phenol aqueous solution.

3.2. Diffusion coefficient of phenol in the crystal pores

Figure 4 plots the absorbance of the OH stretching mode of phenol at 3540 cm^{-1} depending on the time soaked in the phenol solution. The time dependence of the band at 3540 cm^{-1}

corresponds to the diffusion of phenol in the pores of crystal. The absorption was slow and took as long as a few days. The diffusion coefficient (D) can be estimated from the following Fickian equation.

$$\frac{c}{c_0} = \left(\frac{4}{d}\right) \cdot \sqrt{\frac{Dt}{\pi}} \tag{7}$$

Here d is the film thickness, and c and c_0 denote the concentration at time t and the equilibrium state, respectively. The concentration can be replaced by the absorbance using the Lambert-Beer equation (1)

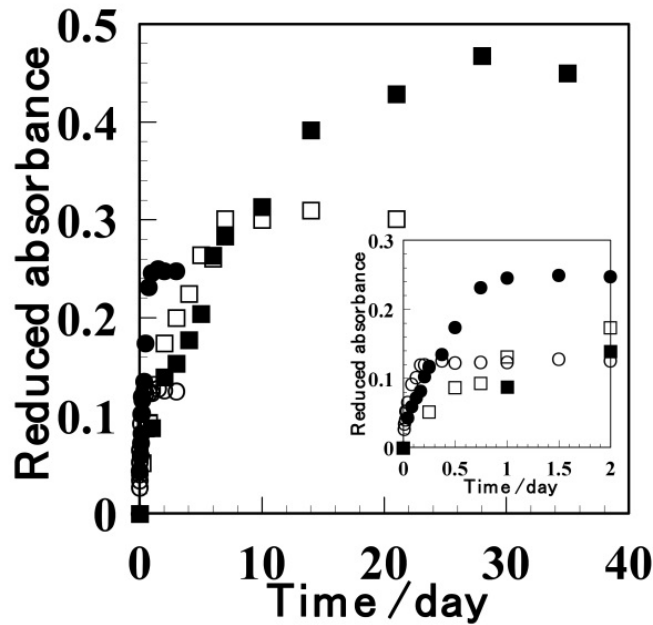$$\frac{I}{I_0} = \left(\frac{4}{d}\right) \cdot \sqrt{\frac{Dt}{\pi}} \tag{8}$$

Figure 4. Absorbance of the OH stretching mode of phenol free from hydrogen bonding depending on the time soaked in a 5 wt% phenol aqueous solution. The ■ and ● notations indicate the cast crystallized and melt-quenched sPS, while □ and ○ represent the cast-crystallized and melt-quenched sPS, respectively. Nakaoki et al.

Here, I_0 and I denote the absorbance at the equilibrium state and the observed absorbance, respectively. Figure 5 plots the normalized intensity I/I_0 against $t^{1/2}$. The diffusion coefficient was estimated from the initial slope and is listed in Table 3. The diffusion coefficient of the cast-crystallized sPPMS was about 4 times larger than that of the cast-crystallized sPS. This can be explained by the large pores present in the sPPMS crystal because of the existence of the methyl group attached to the phenyl group. As for the melt-quenched films, the diffusion was much faster than that of the cast-crystallized films. This is because there is no hindrance, such as transformation of a crystal, to the movement of a phenol molecule. In addition, the non-crystalline chain has a large free volume so that the solvent molecules

tended cause a transformation in the film with ease. When the diffusion of phenol was compared to that of ethanol [33], the diffusion coefficient of phenol is roughly two orders smaller than that of ethanol. This can be interpreted as due to the different molecular size between phenol and ethanol.
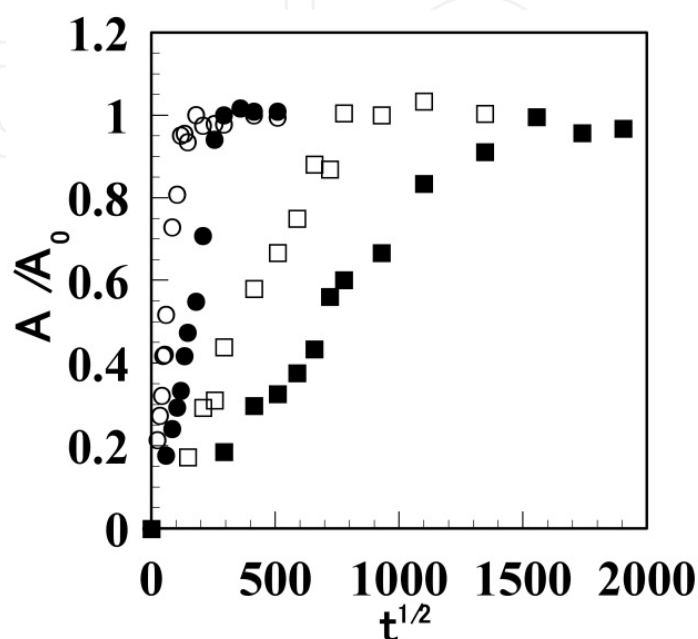

Figure 5. Normalized absorbance of the OH stretching mode of phenol as a function of $t^{1/2}$. The ■ and ● notations indicate the cast-crystallized and melt-quenched sPS and □ and ○ represent the cast-crystallized and melt-quenched sPS, respectively. Nakaoki et al.

	Diffusion coefficient / $\times 10^{-12}$ cm²s⁻¹	Absorbance at the equilibrium state	Concentration / $\times 10^{-4}$ mol cm⁻³	Number of phenol in the pore
sPS/*m*-xylene cast	2.3	0.47	4.37	1.2
sPPMS/*m*-xylene cast	8.2	0.30	2.80	2.0
Melt-quenched sPS	55	0.25	2.12	1.2
Melt-quenched sPPMS	320	0.13	1.23	4.4

Table 3. Diffusion coefficient of phenol in the pore of sPS and sPPMS, and IR absorbance and concentration of phenol at the equilibrium state. The number of phenol molecules in the pores was calculated from the concentration of phenol at the equilibrium state.

It is clear from Fig. 4 that the absorbance became constant after a few tens of days. The absorbance of the 3540 cm⁻¹ band at the equilibrium state is listed in Table 3. The equilibrium

state for the cast-crystallized sPS provided the highest absorbance of these films. This indicates that the incorporation of phenol molecules in the crystal was the largest, corresponding to the high crystallinity of the cast-crystallized δ_e-sPS. The number of phenol molecules in the pores of crystals can be estimated by the absorbance at the equilibrium state. According to Lambert-Beer's law, the absorbance is in proportional to the concentration. In order to estimate the concentration of phenol in the pores of sPS and sPPMS, the absorption coefficient of the hydrogen bond-free OH stretching mode is required. However, normal phenol is hydrogen bonded. So, in order to obtain the required coefficient, each phenol molecule must be isolated from the others. The same problem occurred in the work described in our previous paper which reported the incorporation of ethanol molecules into the pores of cast-crystallized sPS and sPPMS.[34] In that case, the absorption coefficient of the hydrogen bond-free OH stretching mode of ethanol was estimated by diluting the ethanol in toluene. Following this method, toluene was used here as a diluent in order to cancel the interaction between phenol molecules. Figure 6 shows infrared spectra of 5% phenol in aqueous solution, the cast-crystallized sPS film after soaking in phenol solution and a 1 % phenol in toluene solution. The OH stretching mode in the aqueous solution was a broad peak due to hydrogen bonding around 3300 cm^{-1}. However the OH stretching mode diluted by toluene provided a sharp peak at 3540 cm^{-1}, which is identical with that in the pore of cast-crystallized δ_e-sPS. This shows that the phenol is isolated from others by toluene molecules. Therefore the absorption coefficient of the hydrogen bond-free OH stretching mode of phenol was estimated by that of the phenol/toluene solution.
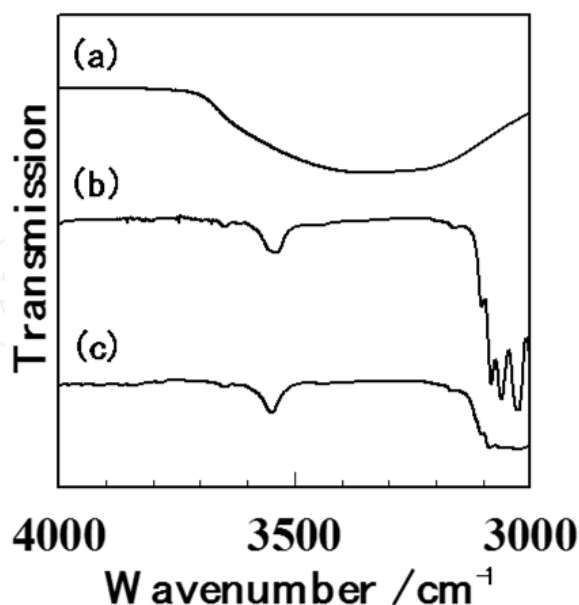

Figure 6. Infrared spectra of the OH stretching mode of phenol: (a) a 5 wt% phenol aqueous solution, (b) cast-crystallized sPS after soaking in 5 wt% phenol aqueous solution, and (c) a 1 v/v% phenol in toluene solution. Nakaoki et al.

Figure 7 plots the absorbance of the OH stretching mode of phenol in the 1 % phenol in toluene solution as a function of path length. The absorption coefficient was estimated to be 2.44×10⁻³. This value was applied to estimate the molar concentration of phenol in the pore of cast-crystallized δₑ-sPS and sPPMS. The molar concentration of phenol at equilibrium state is listed in Table 3. The concentration of phenol in the sPS/m-xylene cast film was the largest of the four films. Since the concentration was estimated from the 3540 cm⁻¹ hydrogen bonding-free band, these solvent molecules were absorbed in the pores of crystal. If the crystallinity is known, the number of phenol molecules in the pores of the crystals can be calculated. So the next section will deal the quantification of phenol molecules in the pores.
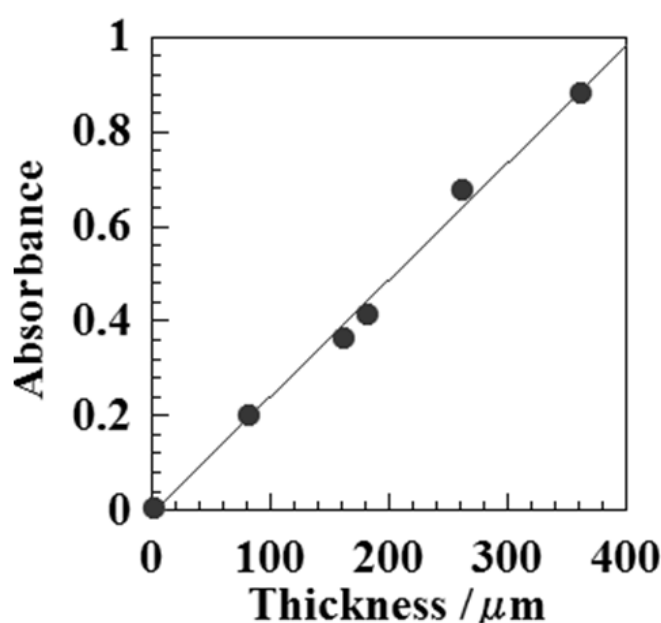

Figure 7. Absorbance of the OH stretching mode of 1 v/v% phenol in toluene as a function of path length. The absorption coefficient was estimated to be 2.44 × 10⁻³ cm²/mol. Nakaoki et al.

3.3. Number of phenol molecules in the pore of sPS

The number of phenol molecules in the pores (n_{phe}) was estimated from the concentration of phenol at the equilibrium state and the crystallinity. The sPS and sPPMS have one pore per four monomer units. As shown in our previous report,[34] the number of phenol molecules trapped in one pore can be estimated by the following equation.

$$n_{phe} = \frac{400 c_{phe}}{c_{poly} \times \chi_c} \tag{9}$$

Here c_{poly} and c_{phe} denote the molar concentrations of polymer and phenol in the pores, respectively. These values were estimated using Lambert-Beer's equation by converting

from the IR absorbance at the equilibrium state. Then the number of phenol molecules incorporated in the pores of sPS and sPPMS was calculated by eq. (9). The crystallinity of cast-crystallized sPS was 0.52 after soaking in phenol solution. When this value is used for the calculation, the number of phenol molecules in the pores was calculated to be 0.34.

Daniel et al. reported that the stoichiometric ratio of the styrene monomeric unit and dichloroethane (DCE) in δ-sPS was 3.6 ± 0.3,[46] which corresponds to 1.1 molecules in one pore of the crystal unit. The number of solvent molecules can be predicted by the relationship between the volume of the solvent molecule and the pore size. Milano et al. reported that one DCE molecule of 0.125 nm^3 is incorporated in the cavity volume of 0.151 nm^3 in the sPS/DCE system.[47] We reported that 1.9 ethanol molecules are incorporated in the pore of cast-crystallized δ$_e$-sPS.[34] Since the volume of ethanol is 0.061 nm^3, 1.9 ethanol molecules can be incorporated in the pore of δ$_e$-sPS with 0.115 nm^3.[46] As the volume of a phenol molecule is 0.10 nm^3, the pore size of cast crystallized δ$_e$-sPS is sufficient for one phenol molecule. Therefore the estimate of the incorporation of 0.34 molecules in one pore must be too small. This might be interpreted as due to the difference between δ$_e$- and δ-sPS. Namely, the δ$_e$-sPS is prepared by evaporating the solvent molecules from δ-sPS, resulting in the pore size becoming smaller after removing the solvent. The pore size for δ$_e$-sPS of 0.115 nm^3 is very close to the volume of a phenol molecule. Therefore the pore size of cast-crystallized δ$_e$-sPS would be too small for a phenol molecule to be incorporated. In fact the crystallinity increased from 38 % to 52 % by soaking in phenol solution. The increase in crystallinity is due to the crystallization to δ-sPS, which is characterized by a complex structure involving sPS and phenol. Therefore, the phenol molecules would be absorbed only in newly crystallized δ-sPS, not in the cast-crystallized δ$_e$-sPS. When the number of phenol molecules is re-calculated using this hypothesis, the result was 1.2 phenol molecules in one pore. Judging from the pore size of δ-sPS, this is a reasonable value.

In the case of melt-quenched sPS film, only δ-sPS is induced during the measurement. The degree of crystallinity increased from 0 to 7.2 %. Since all phenol molecules are incorporated in newly crystallized δ-sPS, the number of phenol molecules in a pore of δ-sPS was calculated to be 1.2, which is identical with the value estimated for the cast-crystallized sPS. Therefore we can conclude that it was impossible for the phenol molecule to be incorporated in the pores of cast-crystallized δ$_e$-sPS, and 1.2 phenol molecules were incorporated in the pore of newly crystallized δ-sPS during the measurement.

3.4. Number of phenol molecules in the pore of sPPMS

In contrast to sPS, sPPMS provided a different result. From the calculation using the crystallinity of 6.5 which corresponds to the value after soaking in phenol solution, the cast-crystallized sPPMS incorporated 2.0 phenol molecules in one pore of the crystal, as shown in Table 3. This is almost twice the number of phenol molecules absorbed in sPS. This is because the pore size of sPPMS is larger than that of sPS because of the methyl group

attached to phenyl ring in sPPMS. According to Tarallo et al.,[32] the clathrate forms of α- and β-classes contain two and one guest molecules in the pore, respectively. They reported that nanoporous sPPMS cast-crystallized from o-xylene forms a α-class clathrate. So, the m-xylene used in this study should induce the formation of α-class crystals. We also reported that 3.8 ethanol molecules were absorbed in the pores of sPPMS.[34] The volume of the phenol molecule is almost twice as large as that of the ethanol molecule. Since the calculation used the crystallinity obtained after soaking in phenol solution, the phenol molecules were incorporated not only in the pores of cast-crystallized sPPMS but also in those of the newly crystallized material. In the case of melt-quenched sPPMS, 4.4 phenol molecules were incorporated in the pore. This value is too high for the pore in sPPMS. In this melt-quenched material, the crystallinity was as low as 1.3 %. The infrared spectrum in Fig. 2(B) shows that the phenol molecule absorbed also in the non-crystalline region. Those phenol molecules would be hydrogen-bonded, but some of them might be isolated from the others. The contribution of these molecules to the 3540 cm^{-1} band will not be negligible. Therefore the number of phenol molecules in the pore might be overestimated; further study on this topic is required.

3.5. Absorption in a mixed solution of phenol and ethanol

In this section, a mixed solution of phenol and ethanol was used to investigate which solvent is preferentially incorporated in the porous crystals of sPS and sPPMS. Figure 8(A) shows the infrared spectra of (a) phenol/ethanol=5/95 mixed solution, (b) the cast-crystallized sPS after soaking in a phenol/ethanol=5/95 mixed solution and (c) the melt-quenched sPS after soaking in the same mixed solution. The OH stretching mode for the mixed solution of phenol and ethanol exhibited a broad peak. This is because there are interactions between the solvents due to hydrogen bonding. The cast-crystallized sPS showed a peak at 3592 cm^{-1}. This wavenumber is not identical with that of phenol at 3540 cm^{-1}. Rather this peak can be assumed to be from ethanol by referencing to our previous paper.[34] This indicates that only ethanol was incorporated in the pores of cast-crystallized δ$_e$-sPS. Since the pore size in the cast-crystallized δ$_e$-sPS is not large enough for phenol molecules, only ethanol molecules would be preferentially incorporated. The phenol is not incorporated in the pore of cast-crystallized δ$_e$-sPS, but is in the newly crystallized δ-sPS. When the melt-quenched sPS was soaked in the mixed solution, a very small peak around 3540 cm^{-1} was observed, indicating that the phenol molecules had induced the formation of δ$_e$-sPS. However most of solvent molecules are settled in the non-crystalline region in which there are interactions due to hydrogen bonding.

Figure 8(B) shows the infrared spectra of (a) phenol/ethanol=5/95 mixed solution, (b) the cast-crystallized sPPMS after soaking in a phenol/ethanol=5/95 mixed solution, and (c), the melt-quenched sPPMS after soaking in the same mixed solution. The hydrogen bond-free OH stretching mode was observed for the cast-crystallized sPS. However, it is worth noting

that two peaks were also observed at 3592 and 3540 cm^{-1}, which are assignable to the OH stretching modes due to ethanol and phenol, respectively. This indicates that both ethanol and phenol were incorporated in the pores of sPPMS. The fact that the pore size in the cast-crystallized sPPMS is large enough for both ethanol and phenol allowed them both to incorporate.
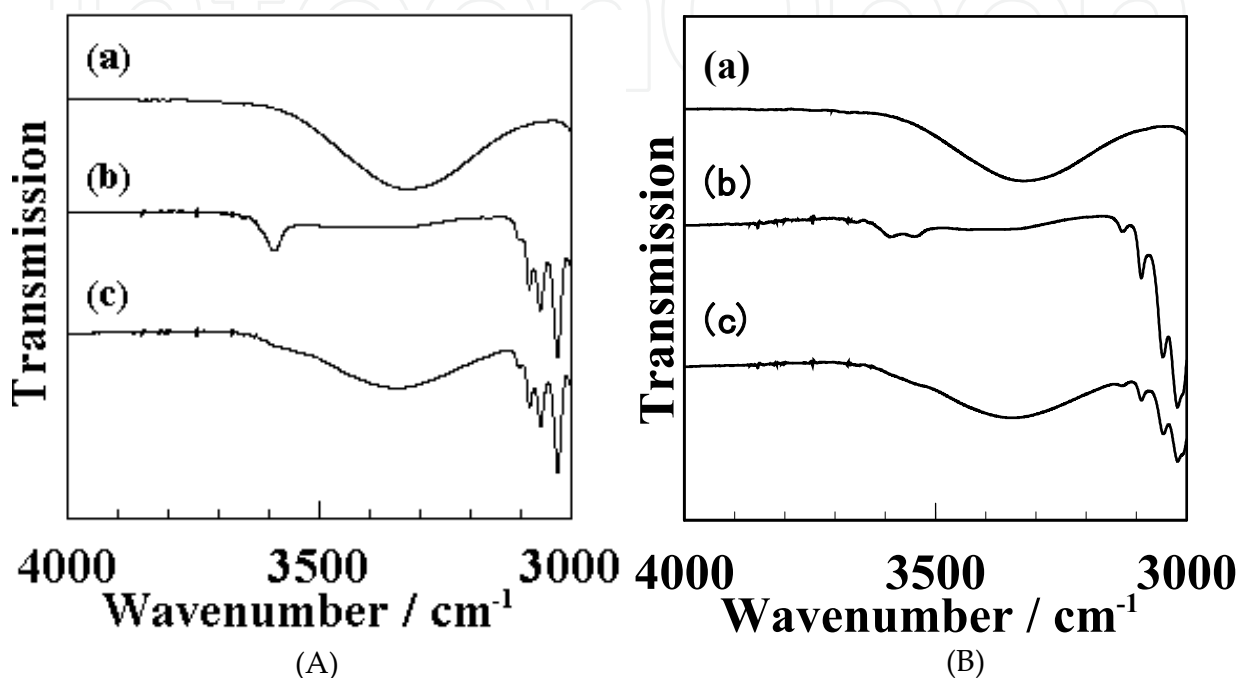

Figure 8. Infrared spectra for the cast-crystallized (a) and melt-quenched (b) sPS (A) and sPPMS (B) after soaking in phenol/ethanol=5/95 for 24 h. The peaks at 3540 cm^{-1} and 3592 cm^{-1} are assignable to the OH stretching mode of phenol and ethanol free from hydrogen bonding, respectively. Nakaoki et al.

In conclusion, sPS preferentially incorporates ethanol, but both ethanol and phenol absorb in sPPMS. This difference resulted from the different pore sizes of sPS and sPPMS.

4. Conclusions

The absorption of phenol into the porous structure of sPS and sPPMS was investigated by infrared spectroscopy. The IR OH stretching mode of phenol for the cast-crystallized sPS and sPPMS films was observed at 3540 cm^{-1}, which corresponds to molecules that are free from hydrogen bonding. This implies that the phenol molecule is isolated from others by incorporation into the nanopores of the crystal. When amorphous films of sPS and sPPMS were soaked in a phenol solution, a hydrogen-bonded peak around 3300 cm^{-1} was observed. This peak was assigned to phenol molecules existing in the non-crystalline phase. In addition, a peak at 3540 cm^{-1} was observed for both sPS and sPPMS, indicating that the formation of a porous crystal was induced by phenol. The diffusion coefficient of

phenol into the pores of cast-crystallized sPPMS was larger than that for the cast-crystallized sPS. This is due to the large pore size of sPPMS resulting from the methyl group attached to the phenyl group of the polymer. In contrast, diffusion in non-crystalline phase was much faster than that in the pores of the crystal. This can be interpreted to mean that no hindrance, such as a crystal, to transport exists in the random chain case. The number of phenol molecules in the pore of a crystal was calculated from the crystallinity and the concentration of phenol in the film. One pore in the cast-crystallized sPS and sPPMS contains 1.2 and 2.0 phenol molecules. It is worth noting that the pore in the δ_e-sPS, which was prepared by casting from *m*-xylene was too small for phenol molecules to be incorporated. Therefore the phenol molecules were only incorporated in newly crystallized δ-sPS during the measurement. In contrast, sPPMS can incorporate solvent not only in the nanoporous crystal, but also in the newly induced crystals because its pores are large enough to accommodate a phenol molecule. When these films were soaked in a mixed solution of phenol/ethanol, the cast-crystallized δ_e-sPS only incorporated ethanol molecules, but the cast-crystallized sPPMS incorporated both phenol and ethanol molecules. This can be explained as due to the small pores in sPS but a large enough space for both molecules in sPPMS.

Author details

Kenichi Furukawa and Takahiko Nakaoki[*]
Department of Materials Chemistry, Ryukoku University, Seta, Otsu, Japan

Acknowledgement

5. References

[1]   Natta G (1955) Une nouvelle classe de polymeres d'α-olefines ayant une régularité de structure exceptionnelle. Journal of Polymer Science 16:143-144.

[2]   Natta G, Pino P, Corradini P, Danusso F, Mantica E, Mazzanti G, Moraglio G (1955) Crystalline High Polymers of α-Olefins. Journal of American Chemical Society 77: 1708-1709.

[3]   Ishihara N, Seimiya T, Kuramoto M, Uoi M (1986) Crystalline syndiotactic polystyrene. Macromolecules 19:2464-2465.

[*] Corresponding Author

[4]   Immirzi A, de Candia F, Ianneli P, Zambelli A, Vittoria V (1988) Solvent-induced polymorphism in syndiotactic polystyrene Makromol. Chem., Rapid Commun. 9: 761-764

[5]   Kobayashi M, Nakaoki T, Ishihara N (1989) Polymorphic Structures and Molecular Vibrations of Syndiotactic Polystyrene. Macromolecules 22: 4377-4382

[6]   De Rosa C, Guerra G, Petraccone V, Corradini P (1991) Crystal Structure of the α-Form of Syndiotactic Polystyrene. *Polymer Journal* 23: 1435-1442

[7]   De Rosa C (1996) Crystal Structure of the Trigonal Modification (α Form) of Syndiotactic Polystyrene. Macromolecules 29: 8460-8465

[8]   Cartier L, Okihara T, Lotz B (1998) The α Superstructure of Syndiotactic Polystyrene: A Frustrated Structure. Macromolecules 31: 3303-3310.

[9]   De Rosa C, Rapacciuolo M, Guerra G, Petraccone V, Corradini P (1992) On the crystal structure of the orthorhombic form of syndiotactic polystyrene. Polymer 33: 1423-1428

[10] Chatani Y, Shimane Y, Ijitsu T, Yukinari T (1993) Structural study on syndiotactic polystyrene: 3. Crystal structure of planar form I. Polymer 34: 1625-1629

[11] Tamai Y, Fukui M (2002) Thermally Induced Phase Transition of Crystalline Syndiotactic Polystyrene Studied by Molecular Dynamics Simulation. Macromolecular Rapid Communications 23: 891-895

[12] Rizzo P, Lamberti M, Albunia A R, Ruiz de Ballesteros O, Guerra G, (2002) Crystalline Orientation in Syndiotactic Polystyrene Cast Films. Macromolecules 35: 5854-5860

[13] Rizzo P, Della Guardia S, Guerra G (2004) Perpendicular Chain Axis Orientation in s-PS Films: Achievement by Guest-Induced Clathrate Formation and Maintenance after Transitions toward Helical and Trans-Planar Polymorphic Forms. Macromolecules 37: 8043-8049

[14] Vittoria V, De Candia F, Ianelli P, Immirizi A (1988) Solvent-induced crystallization of glassy syndiotactic polystyrene. Makromol. Chem. Rapid. Commun. 9: 765-769.

[15] Kobayashi M, Nakaoki T, Ishihara N (1990) Molecular conformation in glasses and gels of syndiotactic and isotactic polystyrenes. Macromolecules 23: 78-83

[16] Guerra G, Musto P, Karasz F E, MacKnight W J (1990) Fourier transform infrared spectroscopy of the polymorphic forms of syndiotactic polystyrene (pages 2111–2119)Makromol. Chem., 191, 2111-2119.

[17] Chatani Y, Shimane Y, Ijitsu T, Yukinari T, Shikuma H (1993) Structural study on syndiotactic polystyrene: 2. Crystal structure of molecular compound with toluene. Polymer 34: 1620-1624

[18] Rizzo P, Daniel C, Girolamo Del Mauro A, Guerra G. (2007) New Host Polymeric Framework and Related Polar Guest Cocrystals. Chem. Mater. 19: 3864-3866

[19] Rizzo P, D'Aniello C, Girolamo Del Mauro A, Guerra G (2007)Thermal Transitions of ε Crystalline Phases of Syndiotactic Polystyrene. Macromolecules 40: 9470 -9474.

[20] Petraccone V, Ruiz O, Tarallo O, Rizzo P, Guerra G (2008) Nanoporous Polymer Crystals with Cavities and Channels. Chem. Mater. 20: 3663-3668

[21] Manfredi C, De Rosa C, Guerra G, Rapacciuolo M, Auriemma F, Corradini P (1995) Structural changes induced by thermal treatments on emptied and filled clathrates of syndiotactic polystyrene. Macromol. Chem. Phys. 196: 2795-2808

[22] Handa Y P, Zhang Z, Wong B (1997) Effect of Compressed CO_2 on Phase Transitions and Polymorphism in Syndiotactic Polystyrene. Macromolecules 30: 8499-8509

[23] Reverchon E, Guerra G, Venditto V (1999) Regeneration of nanoporous crystalline syndiotactic polystyrene by supercritical CO2. J. Applied Polym. Sci. 74: 2077-2082

[24] Nakaoki T, Fukuda Y, Nakajima E, Matsuda T, Harada T (2003) Crystallization Condition of Glassy Syndiotactic Polystyrene in Supercritical CO2. Polymer Journal 35: 430-435

[25] De Rosa C, Guerra G, Petraccone V, Pirozzi B (1997) Crystal Structure of the Emptied Clathrate Form (δ_e Form) of Syndiotactic Polystyrene. *Macromolecules* 30: 4147-4152

[26] De Rosa C, Petraccone V, Guerra G, Manfredi C (1996) Polymorphism of syndiotactic poly(p-methylstyrene): oriented samples. Polymer 37: 5247-5253

[27] De Rosa C, Petraccone V, Dal Poggetto F, Guerra G, Pirrozi B, Di Lorenzo M L, Corradini P (1995) Crystal Structure of Form III of Syndiotactic Poly(p-methylstyrene). Macromolecules, 28: 5507-5511

[28] Ruiz de Ballesteros O, Auriemma F, De Rosa C, Floridi G, Petraccone V (1998) Structural features of the mesomorphic form of syndiotactic poly(p-methylstyrene). Polymer 39: 3523-3528

[29] Dell'Isola A, Floridi G, Rizzo P, Ruiz de Ballesteros O, Petraccone V (1997) On the clathrate forms of syndiotactic poly(*p*-methylstyrene). Macromol. Symp. 114: 243-249

[30] Petraccone V, La Camera D, Caporaso L, De Rosa C (2000) Crystal Structure of the Clathrate Form of Syndiotactic Poly(*p*-methylstyrene) Containing o-Dichlorobenzene. Macromolecules 33: 2610-2615

[31] Petraccone V, La Camera D, Pirrozi B, Rizzo P, De Rosa C, (1998) Crystal Structure of the Clathrate Form of Syndiotactic Poly(p-methylstyrene) Containing Tetrahydrofuran. Macromolecules 31: 5830-5836

[32] Tarallo O, Esposito G, Passarelli U, Petraccone V (2007) A Clathrate Form of Syndiotactic Poly(p-methylstyrene) Containing Two Different Types of Cavities. Macromolecules 40:5471-5478

[33] Petraccone V, Esposito G, Tarallo O, Caporaso L (2005) A New Clathrate Class of Syndiotactic Poly(p-methylstyrene) with a Different Chain Conformation. Macromolecules 38: 5668-5674

[34] Furukawa K, Nakaoki T (2011) Comparison of Absorption Kinetics of Ethanol and Butanol into Different Size Nanopores Present in Syndiotactic Polystyrene and Poly(p-Methylstyrene). Soft Materials 9: 141-153

[35] Manfredi C, Del Nobile M A, Mensitieri G, Guerra G, Rapacciuolo M (1997) Vapor sorption in emptied clathrate samples of syndiotactic polystyrene. J. Polym. Sci. Phys. Ed. 35: 133-140

[36] Venditto V, De Girolamo Del Mauro A, Mensitieri G, Milano G, Musto P, Rizzo P, Guerra G (2006) Anisotropic Guest Diffusion in the δ Crystalline Host Phase of Syndiotactic Polystyrene: Transport Kinetics in Films with Three Different Uniplanar Orientations of the Host Phase. Chem. Mater. 18: 2205-2210

[37] Daniel C, Alfano D, Venditto V, Cardea S, Reverchon E, Larobina D, Mensitieri G, Guerra G (2005) Aerogels with a Microporous Crystalline Host Phase. Adv. Mater. 17: 1515-1518

[38] Daniel C, Sannino D, Guerra G (2008) Syndiotactic Polystyrene Aerogels: Adsorption in Amorphous Pores and Absorption in Crystalline Nanocavities. Chem. Mater. 20: 577-582

[39] Daniel C, Giudice S, Guerra G (2009) Syndiotatic Polystyrene Aerogels with β, γ, and ε Crystalline Phases. Chem. Mater. 21: 1028-1034

[40] Mohri S, Rani D A, Yamamoto Y, Tsujita Y, Yoshimizu H (2004) Structure and properties of the mesophase of syndiotactic polystyrene—III. Selective sorption of the mesophase of syndiotactic polystyrene. J. Polym. Sci., Part B: Polym. Phys. 42: 238-245

[41] Mahesh K P O, Sivakumar M, Yamamoto Y, Tsujita Y, Yoshimizu H, Okamoto S (2004) Structure and properties of the mesophase of syndiotactic polystyrene. VIII. Solvent sorption behavior of syndiotactic polystyrene/p-chlorotoluene mesophase membranes. J. Polym. Sci.: Part B: Polym. Phys. 42: 3439-3446

[42] Sivakumar M, Mahesh K P O, Yamamoto Y, Yoshimizu H, Tsujita Y (2005) Structure and properties of the δ-form and mesophase of syndiotactic polystyrene membranes prepared from different organic solvents. J. Polym. Sci.: Part B: Polym. Phys. 43: 1873-1880

[43] Mahesh K P O, Tsujita Y, Yoshimizu H, Okamoto S, Mohan D J (2005) Study on δ-form complex in syndiotactic polystyrene–organic molecules systems. IV. Formation of complexes with a mixture of solvents and structural changes during the sorption of solvents by syndiotactic polystyrene mesophase membranes. J. Polym. Sci.: Part B: Polym. Phys. 43: 2380-2387

[44] Nakaoki T, Goto N, Saito K (2009) Selective Sorption and Desorption of Organic Solvent for δ-Syndiotactic Polystyrene. Polymer J. 41: 214-218

[45] Nakaoki T, Kobayashi M (2003) Local Conformation of Glassy Polystyrenes with Different Stereoregularity. J. Mol. Struct. 655: 343-349

[46] Daniel C, Guerra G, Musto P (2002) Clathrate Phase in Syndiotactic Polystyrene Gels. Macromolecules 35: 2243-2251

[47] Milano G, Venditto V, Guerra G, Cavallo L, Ciambelli P, Sannino D (2001) Shape and Volume of Cavities in Thermoplastic Molecular Sieves Based on Syndiotactic Polystyrene. Chem. Mater. 13: 1506-1511